

How Vintage Linear Systems Controllers Have Become Inadequate In Renewables-Heavy Power Systems: Limitations and New Solutions

Sebastian A. Nugroho[†] and Ahmad F. Taha[‡]

Abstract—In power systems, various control engineering algorithms are instrumented to regulate voltages and frequencies. One of these algorithms is load frequency control (LFC). Thanks to developments in control theory and convex optimization, numerous LFC strategies have been proposed. However, many rely on a reduced, linearized model of power systems where: (i) load and renewables buses are eliminated, (ii) only synchronous machines are modeled, (iii) nonlinear network transients are replaced with their linear approximations around tight operating regions, and (iv) algebraic power flows are eliminated. In contrast, the increased penetration of renewables from wind and solar introduces significant uncertainty which can only be captured explicitly via a nonlinear differential algebraic equation (NDAE) model that incorporates loads, renewables, and nonlinear machine and power flow transients. As it is demonstrated herein, such vintage, linearization-based approaches may be inadequate. They can be easily overwhelmed by high degree of uncertainty, thereby failing to stabilize power systems post-disturbance. To that end, we showcase the limitations of some widely utilized linearization-based LFC methods and offer a new solution which manifests through a simple, linearization-free approach that can handle large disturbances in power systems originating from a sudden reduction of renewables generation and increase of demands.

Keywords—Power systems, load frequency control, differential algebraic equations, linear quadratic regulator, robust \mathcal{H}_∞ control.

I. INTRODUCTION

FREQUENCY regulation constitutes one of the main control problems in modern multi-machine power systems. The *load frequency control* (LFC) problem is associated with the capability to preserve the power balance between the total generated power against the total load demand [1] in near real-time. Future, renewables-dominant power systems face great challenges due to the increased participation of renewable energy resources especially wind and photovoltaic (PV) solar farms. The high variability of electric power generated by renewables, in addition to load fluctuations, makes frequency regulation even more challenging.

Several approaches have been proposed in the literature to provide frequency regulation services. In multi-area power networks, automatic generation control (AGC) is a secondary, inter-area control architecture that regulates the network's frequency as well as the interchange of power flows [2]; note that AGC and LFC can be used interchangeably. AGC commonly implements conventional/classical controllers to control the turbine governor such that the total area control error (ACE) is minimized. The developments of convex optimization methods encourage the design of more advanced control strategies particularly for power system applications. Many optimal control methods have been proposed accordingly, e.g., to perform LFC in a two-area power systems [3], [4]. A recent

study conducted in [5] investigates the joint optimal power flow problem with LFC using linear quadratic regulator (LQR). A robust H_∞ LFC method for an interconnected two-area power systems is developed in [6] to specifically handle disturbances from the tie-line interconnections. As a departure from the H_∞ control, the concept of \mathcal{L}_∞ stability is utilized in [7] to implement a robust control architecture for LFC. The behavior of power networks pertaining to the increasing penetration of distributed energy resources (DERs) including renewables is recently studied in [8], where the authors showcase how power system control becomes *harder* (in the control-theoretic sense) as more renewable energy is added.

It is noteworthy that the majority of these approaches rely on power systems models linearized with respect to a certain operating point—we refer to such controllers as *linearization-based controllers*. As such, the resulting stability and performance guarantees only apply on confined neighborhoods around the operating point. This simply follows from linear dynamic systems theory. Furthermore, and to derive such linearization-based controllers, the algebraic equations that govern network power flows are eliminated and only the dynamics of the generators (through linear differential equations) are captured. This results in only penalizing deviations from the nominal operating point of the dynamic states of generators—the algebraic states (i.e., voltages and currents) are hence not explicitly controlled.

With that in mind, many studies [5], [7]–[9] have demonstrated that when applying the linearization-based controller to the more comprehensive, nonlinear differential algebraic equation (NDAE) model of power network, such controllers are able to stabilize both dynamic generator and algebraic states. One might add that this is a fortunate coincidence, as the aforementioned linear systems theory is not designed to guarantee stabilization NDAE models. Consequently, a significant disturbance—for instance, due to uncertainties induced by faults and the variability of renewables and loads—may be strong enough to kick the system out of the desired operating region. This implies that a controller gain matrix (computed as a function of the original operating point) has to be updated whenever a large disturbance moves the network to a different operating region. Although there exist some LFC strategies that do not involve any linearization, e.g. [2], [10] only equations pertaining to generator buses and active power flows are considered to derive the controller gains.

The paper's objective is two-fold: (i) to showcase the limitations of traditional linear systems theory tools in performing LFC in the presence of disturbances from renewables; (ii) to offer a new linearization-free controller that is more robust despite being as simple as its aforementioned counterparts. Towards that end goal, the paper's contributions are:

- Through numerical simulations, we demonstrate that vintage linearization-based methods, specifically LQR, AGC, and \mathcal{H}_∞

[†]Department of Electrical and Computer Engineering, University of Michigan, Ann Arbor, MI 48109. [‡]Department of Civil and Environmental Engineering, Vanderbilt University, Nashville, TN 37235. Emails: snugroho@umich.edu, ahmad.taha@vanderbilt.edu. This work is supported by the National Science Foundation under Grant 2151571 and 2152450.

controllers when implemented to perform LFC on an NDAE model of power networks, could perform poorly and eventually fail to stabilize the network even under moderate disturbances.

- We propose a novel linearization-free controller, derived based on the NDAE models of power networks, which controller gain can be computed by solving a convex optimization problem involving linear matrix inequalities (LMIs).
- We show the superiority of the proposed linearization-free controller against LQR, AGC, and \mathcal{H}_∞ controllers in maintaining system-wide frequency on the event of sudden changes in renewables generation and power demands.

The remainder of the paper is organized as follows. Section II presents the NDAE models of power networks while Section III reviews the most common linear systems theory-based control algorithms. Section IV discusses the design of the proposed state feedback control strategy for the stabilization of NDAE models of power systems. Thorough numerical studies are provided in Section V. The paper is concluded in Section VI.

II. DYNAMICS OF MULTI-MACHINE POWER SYSTEMS

We consider a power network consisting N number of buses, modeled by a graph $(\mathcal{N}, \mathcal{E})$ where \mathcal{N} is the set of nodes and \mathcal{E} is the set of edges. Note that \mathcal{N} consists of traditional synchronous generator, renewable energy resources, and load buses, i.e., $\mathcal{N} = \mathcal{G} \cup \mathcal{R} \cup \mathcal{L}$ where \mathcal{G} collects G generator buses, \mathcal{R} collects the buses containing R renewables, while \mathcal{L} collects L load buses. The 4th-order dynamics of synchronous generators are given as [11]

$$\dot{\delta}_i = \omega_i - \omega_0 \quad (1a)$$

$$M_i \dot{\omega}_i = T_{Mi} - P_{Gi} - D_i(\omega_i - \omega_0) \quad (1b)$$

$$T'_{d0i} \dot{E}'_i = -\frac{x_{di}}{x'_{di}} E'_i + \frac{x_{di} - x'_{di}}{x'_{di}} v_i \cos(\delta_i - \theta_i) + E_{fdi} \quad (1c)$$

$$T_{CHi} \dot{T}_{Mi} = -T_{Mi} - \frac{1}{R_{Di}} (\omega_i - \omega_0) + T_{ri}. \quad (1d)$$

where $\delta_i, \omega_i, E'_i, T_{Mi}$ are generator's internal states and E_{fdi}, T_{ri} are generator's inputs. Despite that these states and inputs are time-varying, its time dependence indicator (t) is dropped here for brevity (we do this in the subsequent sections to save space). The constant terms in (1) are as follows: M_i is the rotor's inertia constant ($\text{pu} \times s^2$), D_i is the damping coefficient ($\text{pu} \times s$), x_{di} is the direct-axis synchronous reactance (pu), x'_{di} is the direct-axis transient reactance (pu), T'_{d0i} is the direct-axis open-circuit time constant (s), T_{CHi} is the chest valve time constant, R_{Di} is the regulation constant for the speed-governing mechanism, and ω_0 denotes the rotor's synchronous speed (rad/s). The relations among generator's internal states $(\delta_i, \omega_i, E'_i, T_{Mi})$, generator's supplied power (P_{Gi}, Q_{Gi}) , and terminal voltage \bar{v}_i are given by [7]

$$P_{Gi} = \frac{1}{x'_{di}} E'_i v_i \sin(\delta_i - \theta_i) - \frac{x_{qi} - x'_{di}}{2x'_{di} x_{qi}} v_i^2 \sin(2(\delta_i - \theta_i)) \quad (2a)$$

$$Q_{Gi} = \frac{1}{x'_{di}} E'_i v_i \cos(\delta_i - \theta_i) - \frac{x'_{di} + x_{qi}}{2x'_{di} x_{qi}} v_i^2 - \frac{x_{qi} - x'_{di}}{2x'_{di} x_{qi}} v_i^2 \cos(2(\delta_i - \theta_i)). \quad (2b)$$

The power flow equations, for $i \in \mathcal{G} \cap \mathcal{R} \cap \mathcal{L}$, representing the distribution of real and reactive power are [11]

$$P_{Gi} + P_{Ri} + P_{Li} = \sum_{j=1}^N v_i v_j (G_{ij} \cos \theta_{ij} + B_{ij} \sin \theta_{ij}) \quad (3a)$$

$$Q_{Gi} + Q_{Ri} + Q_{Li} = \sum_{j=1}^N v_i v_j (G_{ij} \sin \theta_{ij} - B_{ij} \cos \theta_{ij}), \quad (3b)$$

where $\theta_{ij} := \theta_i - \theta_j$. In (3), (P_{Ri}, Q_{Ri}) denote the active and reactive power generated by renewables, while (P_{Li}, Q_{Li}) denote the active and reactive power consumed by the loads. In order to construct the nonlinear state-space representation of the multi-machine power networks (1)-(3), define \mathbf{x}_d as the vector populating all dynamic states of the network such that $\mathbf{x}_d := [\delta^\top \omega^\top E'^\top T_M^\top]^\top$ in which $\delta := \{\delta_i\}_{i \in \mathcal{G}}$, $\omega := \{\omega_i\}_{i \in \mathcal{G}}$, $E' := \{E'_i\}_{i \in \mathcal{G}}$, $T_M := \{T_{Mi}\}_{i \in \mathcal{G}}$; \mathbf{a} as the algebraic state corresponding to generator's power such that $\mathbf{a} := [P_G^\top Q_G^\top]^\top$ where $P_G := \{P_{Gi}\}_{i \in \mathcal{G}}$, $Q_G := \{Q_{Gi}\}_{i \in \mathcal{G}}$; and $\tilde{\mathbf{v}}$ as the algebraic state representing the network's complex bus voltages such that $\tilde{\mathbf{v}} := [\mathbf{v}^\top \theta^\top]^\top$ where $\mathbf{v} := \{v_i\}_{i \in \mathcal{N}}$, $\theta := \{\theta_i\}_{i \in \mathcal{N}}$. The input of the system is considered to be $\mathbf{u} := [E_{fd}^\top T_r^\top]^\top$ where $E_{fd} := \{E_{fdi}\}_{i \in \mathcal{G}}$ and $T_r := \{T_{ri}\}_{i \in \mathcal{G}}$. In addition, define the vector \mathbf{q} as $\mathbf{q} := [P_R^\top Q_R^\top P_L^\top Q_L^\top]^\top$ where $P_R := \{P_{Ri}\}_{i \in \mathcal{R}}$, $Q_R := \{Q_{Ri}\}_{i \in \mathcal{R}}$, $P_L := \{P_{Li}\}_{i \in \mathcal{L}}$, $Q_L := \{Q_{Li}\}_{i \in \mathcal{L}}$. The above notations allow (1)-(3) to be written into a compact, nonlinear differential algebraic equation (NDAE) state space model:

$$\text{NDAE: } \dot{\mathbf{x}}_d = \mathbf{A}_d \mathbf{x}_d + \mathbf{G}_d \mathbf{f}_d(\mathbf{x}_d, \mathbf{x}_a) + \mathbf{B}_d \mathbf{u} + \mathbf{h} \omega_0 \quad (4a)$$

$$0 = \mathbf{A}_a \mathbf{x}_a + \mathbf{G}_a \mathbf{f}_a(\mathbf{x}_d, \mathbf{x}_a) + \mathbf{B}_a \mathbf{q}, \quad (4b)$$

where $\mathbf{x}_d \in \mathbb{R}^{nd}$, $\mathbf{x}_a := [\mathbf{a}^\top \tilde{\mathbf{v}}^\top]^\top \in \mathbb{R}^{na}$, $\mathbf{u} \in \mathbb{R}^{nu}$, and $\mathbf{q} \in \mathbb{R}^{nq}$. The functions $\mathbf{f}_d : \mathbb{R}^{nd} \times \mathbb{R}^{na} \rightarrow \mathbb{R}^{nfd}$, $\mathbf{f}_a : \mathbb{R}^{nd} \times \mathbb{R}^{na} \rightarrow \mathbb{R}^{nf_a}$, constant matrices $\mathbf{A}_d \in \mathbb{R}^{nd \times nd}$, $\mathbf{A}_a \in \mathbb{R}^{na \times na}$, $\mathbf{G}_d \in \mathbb{R}^{nfd \times nd}$, $\mathbf{G}_a \in \mathbb{R}^{nf_a \times na}$, $\mathbf{B}_d \in \mathbb{R}^{nu \times nd}$, $\mathbf{B}_a \in \mathbb{R}^{nq \times na}$, and vector $\mathbf{h} \in \mathbb{R}^{nd}$ are all detailed in Appendix A of [12].

Notice that the state space equation (4) represents the NDAEs of power networks, which cannot be utilized by linearization-based controllers. To that end, we perform linearization to (4) using the first order Taylor approximation to obtain a linear model. Let $\delta_i^0, \omega_i^0, e_{di}^0, P_{Gi}^0, Q_{Gi}^0, T_{Mi}^0, E_{fdi}^0$ for $i \in \mathcal{G}$, $P_{L,i}^0$ and $Q_{L,i}^0$ for $i \in \mathcal{L}$, $P_{R,i}^0$ and $Q_{R,i}^0$ for $i \in \mathcal{R}$, and \tilde{v}_i^0 for $i \in \mathcal{N}$ be the operating point of the system. Linearizing (4) around this point gives the following equations

$$\Delta \dot{\mathbf{x}}_d = \tilde{\mathbf{A}}_{dd} \Delta \mathbf{x}_d + \tilde{\mathbf{A}}_{da} \Delta \mathbf{x}_a + \mathbf{B}_d \Delta \mathbf{u} \quad (5a)$$

$$0 = \tilde{\mathbf{A}}_{ad} \Delta \mathbf{x}_d + \tilde{\mathbf{A}}_{aa} \Delta \mathbf{x}_a + \mathbf{B}_a \Delta \mathbf{q}, \quad (5b)$$

where $\Delta \mathbf{x}_d := \mathbf{x}_d - \mathbf{x}_d^0$, $\Delta \mathbf{x}_a := \mathbf{x}_a - \mathbf{x}_a^0$, $\Delta \mathbf{u} := \mathbf{u} - \mathbf{u}^0$, and $\Delta \mathbf{q} := \mathbf{q} - \mathbf{q}^0$, which respectively denote the deviations of the current dynamic state \mathbf{x}_d , algebraic state \mathbf{x}_a , input \mathbf{u} , and renewable-load power \mathbf{q} to the given operating point $(\mathbf{x}_d^0, \mathbf{x}_a^0, \mathbf{u}^0, \mathbf{q}^0)$. Assuming that $\tilde{\mathbf{A}}_{aa}$ is a nonsingular matrix (see [13]), the linear DAE (5) can be reduced to a linearized ordinary differential (LODE) state space model

$$\text{LODE: } \Delta \dot{\mathbf{x}}_d = \tilde{\mathbf{A}} \Delta \mathbf{x}_d + \mathbf{B}_d \Delta \mathbf{u} + \tilde{\mathbf{B}}_a \Delta \mathbf{q}, \quad (6)$$

where $\tilde{\mathbf{A}} := \tilde{\mathbf{A}}_{dd} - \tilde{\mathbf{A}}_{da} \tilde{\mathbf{A}}_{aa}^{-1} \tilde{\mathbf{A}}_{ad}$ and $\tilde{\mathbf{B}}_a := -\tilde{\mathbf{A}}_{da} \tilde{\mathbf{A}}_{aa}^{-1} \mathbf{B}_a$. The equation in (6) describes the dynamical behavior of the network around the given operating point. It is noteworthy that: (1) the algebraic state $\Delta \mathbf{x}_a$ is eliminated while the dynamic state $\Delta \mathbf{x}_d$

remains and (2) the linearized model (6) *does* depend on the operating point while the nonlinear DAE (4) does *not*.

III. LINEARIZATION-BASED APPROACHES FOR LFC

The power generated by renewables and consumed by loads are inherently time-varying and highly fluctuating. Although these power figures follow some certain patterns (e.g., daily aggregate power consumption of residential buildings, seasonal weather patterns), precise prediction on minute-to-minute basis is still difficult to perform. Indeed, the scheduling of synchronous generators—that is, determining the amount of power that needs to be produced—is dependent on the available day-ahead loads and renewables forecasts, which provide hourly figures of power demand and production [14]. Provided with such information, the independent system operator solves the power flow (PF) or optimal power flow (OPF) problem repeatedly for every certain time interval, typically 15 minutes [15]—this is referred to as the dispatch period. The resulting solutions are then employed to aid primary, secondary and tertiary controls [15]. Let \mathbf{q}^k be the predicted demand and renewable generation at the k -th dispatch period. Since $\mathbf{q}(t)$ fluctuates, then at any time instance, it will be likely that $\mathbf{q}^k \neq \mathbf{q}(t)$. The difference between \mathbf{q}^k (prediction) and $\mathbf{q}(t)$ (actual) acts as a disturbance on the power system. In the LODE model, $\Delta\mathbf{q}$ represents this particular disturbance and thus, the objective of the controller is to provide control action $\Delta\mathbf{u}$ that minimizes the deviation of frequency $\omega_i - \omega_0$ for all $i \in \mathcal{G}$. The next section summarizes two LFC methods, that determine $\Delta\mathbf{u}(t)$ essentially, which utilize linearized ODE representations of power networks.

A. The Linear-Quadratic Regulator (LQR)

Consider a simplified representation of (6) with $\Delta\mathbf{q} = 0$ (that is, the disturbance is assumed to be absent)

$$\dot{\mathbf{x}}_d(t) = \tilde{\mathbf{A}}\Delta\mathbf{x}_d(t) + \mathbf{B}_d\Delta\mathbf{u}(t), \quad (7)$$

where $\Delta\mathbf{x}_d \in \mathbb{R}^n$ and $\Delta\mathbf{x}_{d,0} = \Delta\mathbf{x}_d(t_0)$ is the corresponding initial condition. The optimal control problem seeks for the best (optimal) control action $\Delta\mathbf{u} \in \mathbb{R}^m$ for all $t \geq 0$ that minimizes a certain predefined cost. For that purpose, it is assumed that the pair $(\tilde{\mathbf{A}}, \mathbf{B}_d)$ is controllable. Using a linear state feedback control policy $\Delta\mathbf{u} = \mathbf{K}\Delta\mathbf{x}_d$ where $\mathbf{K} \in \mathbb{R}^{m \times n}$ is the controller gain matrix, the optimal control problem can be reduced to the search of stabilizing \mathbf{K} that minimizes

$$J_\infty := \int_{t_0}^{\infty} \Delta\mathbf{x}_d^\top(t) \mathbf{Q} \Delta\mathbf{x}_d(t) + \Delta\mathbf{u}^\top(t) \mathbf{R} \Delta\mathbf{u}(t) dt, \quad (8)$$

where $\mathbf{Q} \succeq 0$ and $\mathbf{R} \succ 0$ are weight matrices for the state and input. It is known that the optimal solution of such problem can be obtained by solving the continuous-time, Algebraic Riccati Equation (ARE)

$$\tilde{\mathbf{A}}^\top \mathbf{P} + \mathbf{P} \tilde{\mathbf{A}} - \mathbf{P} \mathbf{B}_d \mathbf{R}^{-1} \mathbf{B}_d^\top \mathbf{P} + \mathbf{Q} = 0, \quad (9)$$

for some $\mathbf{P} \succ 0$ [16]. The optimal control gain is then given by $\mathbf{K} = -\mathbf{R}^{-1} \mathbf{B}_d^\top \mathbf{P}$ with minimum cost $J_\infty = \Delta\mathbf{x}_{d,0}^\top \mathbf{P} \Delta\mathbf{x}_{d,0}$.

B. Robust \mathcal{H}_∞ Control

The robust \mathcal{H}_∞ control is mainly employed to control systems in which disturbances are explicitly taken into account. Now consider

an extension of LODE (6) with controlled output $\mathbf{z} \in \mathbb{R}^z$ written as

$$\dot{\mathbf{x}}_d(t) = \tilde{\mathbf{A}}\Delta\mathbf{x}_d(t) + \mathbf{B}_d\Delta\mathbf{u}(t) + \tilde{\mathbf{B}}_a\Delta\mathbf{q}(t), \quad (10a)$$

$$\mathbf{z}(t) = \mathbf{Z}_x\Delta\mathbf{x}_d(t) + \mathbf{Z}_u\Delta\mathbf{u}(t), \quad (10b)$$

where \mathbf{Z}_x and \mathbf{Z}_u are user-designed weighting matrices with appropriate dimensions. For simplicity, a linear full state feedback control policy $\Delta\mathbf{u} = \mathbf{K}\Delta\mathbf{x}_d$ where $\mathbf{K} \in \mathbb{R}^{m \times n}$ is considered. Using Linear Fractional Transformation (LFT) [17], it can be shown that the transfer function of system (10) from $\Delta\mathbf{q}(s)$ to $\mathbf{z}(s)$, where $s \in \mathbb{C}$ is the complex Laplace variable, can be expressed as

$$\mathbf{G}(s) = \begin{bmatrix} \tilde{\mathbf{A}} + \mathbf{B}_d \mathbf{K} & \tilde{\mathbf{B}}_a \\ \mathbf{Z}_x + \mathbf{Z}_u \mathbf{K} & \mathbf{O} \end{bmatrix}.$$

Assuming that there exists such \mathbf{K} such that the system $\mathbf{G}(s)$ is stable, the \mathcal{H}_∞ norm of $\mathbf{G}(s)$ is defined as the \mathcal{L}_2 -induced norm of the input-output operator $\mathbf{G}: \Delta\mathbf{q} \rightarrow \mathbf{z}$ such that

$$\|\mathbf{G}\|_{\mathcal{H}_\infty} := \sup_{\Delta\mathbf{q} \in \mathcal{L}_2} \left\{ \frac{\|\mathbf{z}\|_{\mathcal{L}_2}}{\|\Delta\mathbf{q}\|_{\mathcal{L}_2}}, \Delta\mathbf{q} \neq 0 \right\}.$$

It can be shown from the bounded-real lemma [18] that the \mathcal{H}_∞ norm of the closed-loop system $\mathbf{G}(s)$ is minimized and bounded by $\gamma > 0$ if there exists a solution to the problem

$$\text{minimize}_{\gamma, \mathbf{P}, \mathbf{X}} \gamma \quad (11a)$$

$$\text{s.t. } \begin{bmatrix} \tilde{\mathbf{A}}\mathbf{P} + \mathbf{P}\tilde{\mathbf{A}}^\top + \mathbf{X}^\top \mathbf{B}_d^\top + \mathbf{B}_d \mathbf{X} & * & * \\ \tilde{\mathbf{B}}_a^\top & -\gamma \mathbf{I} & * \\ \mathbf{Z}_x \mathbf{P} + \mathbf{Z}_u \mathbf{X} & \mathbf{O} & -\gamma \mathbf{I} \end{bmatrix} \prec 0 \quad (11b)$$

$$\mathbf{P} \succ 0, \gamma > 0. \quad (11c)$$

After the problem given in (11) is solved, the optimal controller gain matrix can be computed as $\mathbf{K} = \mathbf{X}\mathbf{P}^{-1}$.

IV. A NEW LINEARIZATION-FREE CONTROLLER

The goal of the linearization-free controller is to maintain frequency stability of the system despite the unpredictable, uncontrollable variations of power generated by renewables as well as power demands. However, this particular controller uses the power network's NDAE model (4). Let \mathbf{q}^k be the predicted power generated by the renewables as well as the predicted power consumed by the loads during the k -th dispatch period—that is, for any time t such that $kT \leq t \leq (k+1)T$ for a fixed $T > 0$, which is typically 15 minutes [15]. This quantity is available for most system operators and is routinely published online. Let $\mathbf{u}_{\text{ref}}^k$ be the reference (baseline) input for the generators which, for a given prediction of renewables and demands \mathbf{q}^k , brings the power system (4) to the predicted operating point during this time period. Define $(\mathbf{x}_d^k, \mathbf{x}_a^k)$ as the corresponding steady state dynamic and algebraic states. By defining \mathbf{u}_{LFC} as the proposed control input during the k -th dispatch period such that

$$\mathbf{u}_{\text{LFC}} := \mathbf{u}_{\text{LRFC}}(t) = \mathbf{u}_{\text{ref}}^k + \mathbf{K}_d(\mathbf{x}_d(t) - \mathbf{x}_d^k),$$

the power network's dynamics (4) with the proposed control framework can be written as

$$\dot{\mathbf{x}}_d = \mathbf{A}_d \mathbf{x}_d + \mathbf{G}_d \mathbf{f}_d(\mathbf{x}_d, \mathbf{x}_a) + \mathbf{B}_d \mathbf{u}_{\text{LFC}} + \mathbf{h}\omega_0 \quad (12a)$$

$$\mathbf{0} = \mathbf{A}_a \mathbf{x}_a + \mathbf{G}_a \mathbf{f}_a(\mathbf{x}_d, \mathbf{x}_a) + \mathbf{B}_a \mathbf{q}, \quad (12b)$$

where $\mathbf{K}_d \in \mathbb{R}^{n_u \times n_d}$ is the corresponding controller gain matrix. The design of gain \mathbf{K}_d is given later in this section.

Now define the states $\tilde{\mathbf{x}}_d \in \mathbb{R}^{n_d}$ and $\tilde{\mathbf{x}}_a \in \mathbb{R}^{n_a}$ as the deviations of the dynamic and algebraic states of the perturbed system around $(\mathbf{x}_d^k, \mathbf{x}_a^k)$, respectively, and they are given as $\tilde{\mathbf{x}}_d := \mathbf{x}_d - \mathbf{x}_d^k$ and $\tilde{\mathbf{x}}_a := \mathbf{x}_a - \mathbf{x}_a^k$. From (12) and letting $\tilde{\mathbf{q}} := \mathbf{q} - \mathbf{q}^k$, the perturbed network's dynamics can be derived as

$$\dot{\tilde{\mathbf{x}}}_d = (\mathbf{A}_d + \mathbf{B}_d \mathbf{K}_d) \tilde{\mathbf{x}}_d + \mathbf{G}_d \tilde{\mathbf{f}}_d(\tilde{\mathbf{x}}_d, \tilde{\mathbf{x}}_a) \quad (13a)$$

$$\mathbf{0} = \mathbf{A}_a \Delta \mathbf{x}_a + \mathbf{G}_a \tilde{\mathbf{f}}_a(\tilde{\mathbf{x}}_d, \tilde{\mathbf{x}}_a) + \mathbf{B}_a \tilde{\mathbf{q}}, \quad (13b)$$

where the mapping $\tilde{\mathbf{f}}_d(\cdot)$ is nothing but $\tilde{\mathbf{f}}_d(\tilde{\mathbf{x}}_d(t), \tilde{\mathbf{x}}_a(t)) := \mathbf{f}_d(\mathbf{x}_d(t), \mathbf{x}_a(t)) - \mathbf{f}_d(\mathbf{x}_d^k, \mathbf{x}_a^k)$ (likewise for $\tilde{\mathbf{f}}_a(\cdot)$). In (13), $\tilde{\mathbf{q}}$ represents the deviations of the current demand and renewables generation \mathbf{q} from the predicted value \mathbf{q}^k during this dispatch period. Our objective herein is to design the gain matrix \mathbf{K}_d such that all trajectories of the solutions of the NDAE (13) converge asymptotically towards the zero equilibrium of (13), despite the presence of nonzero disturbance caused by $\tilde{\mathbf{q}}$ (that is, the mismatch between the predicted and the actual power from renewables and loads). Note that (a) the shifting of the coordinates is performed for theoretical convenience—the proposed controller is *not* operating-point or linearization dependent and (b) the proposed controller is designed assuming an ideal case, i.e., the disturbance is assumed to be zero such that $\tilde{\mathbf{q}} = \mathbf{0}$. Despite this assumption, in Section V we assess the performance of the proposed controller in performing LFC against a significant nonzero disturbance.

Let us define \mathcal{X}_d and \mathcal{X}_a as the sets representing the operating region(s) of the system and describe the solution manifold of (13) such that $\tilde{\mathbf{x}}_d \in \mathcal{X}_d \subseteq \mathbb{R}^{n_d}$ and $\tilde{\mathbf{x}}_a \in \mathcal{X}_a \subseteq \mathbb{R}^{n_a}$. Assuming that the functions $\tilde{\mathbf{f}}_d(\cdot)$ and $\tilde{\mathbf{f}}_a(\cdot)$ are bounded for all $\tilde{\mathbf{x}}_d \in \mathcal{X}_d$ and $\tilde{\mathbf{x}}_a \in \mathcal{X}_a$ and the NDAE (12) is of index one [12], the stabilizing controller gain matrix \mathbf{K}_d can be synthesized by solving the following optimization problem with LMIs [12]

$$(\mathbf{P}) \underset{\bar{\epsilon}, \mathbf{X}_1, \mathbf{X}_2, \mathbf{R}, \mathbf{Y}, \mathbf{W}}{\text{minimize}} \kappa \|\mathbf{W}\|_2 \quad (14a)$$

$$\text{subject to } \mathbf{X}_1 \succ 0, \bar{\epsilon} > 0, \quad (14b)$$

$$\begin{bmatrix} \Psi & * & * & * \\ \mathbf{A}_a \mathbf{X}_2 \mathbf{E}_d^\top + \mathbf{A}_d \mathbf{Y} & \Theta & * & * \\ \bar{\mathbf{H}}_d^{\frac{1}{2}} \mathbf{X}_1 \mathbf{E}_d^\top & \mathbf{O} & -\bar{\epsilon} \mathbf{I} & * \\ \bar{\mathbf{H}}_a^{\frac{1}{2}} \mathbf{X}_2 \mathbf{E}_d^\top + \bar{\mathbf{H}}_a^{\frac{1}{2}} \mathbf{Y} & \bar{\mathbf{H}}_d^{\frac{1}{2}} \mathbf{R} & \mathbf{O} & -\bar{\epsilon} \mathbf{I} \end{bmatrix} \prec 0, \quad (14c)$$

where:

- the variables in (14) are positive definite matrix $\mathbf{X}_1 \in \mathbb{S}_{++}^{n_d}$, and real-valued matrices $\mathbf{X}_2 \in \mathbb{R}^{n_a \times n_d}$, $\mathbf{R} \in \mathbb{R}^{n_a \times n_a}$, $\mathbf{Y} \in \mathbb{R}^{n_d \times n_a}$, $\mathbf{W} \in \mathbb{R}^{n_u \times n_d}$, and scalar $\bar{\epsilon} \in \mathbb{R}_{++}$;
- the scalar $\kappa \in \mathbb{R}_{++}$ is a predefined constant whereas $\|\mathbf{W}\|_2$ denotes the induced 2-norm of matrix \mathbf{W} ;
- matrices Ψ and Θ are given as

$$\begin{aligned} \Psi &:= \mathbf{E}_d \mathbf{X}_1 \mathbf{A}_d^\top + \mathbf{A}_d \mathbf{X}_1 \mathbf{E}_d^\top \\ &\quad + \mathbf{E}_d \mathbf{W}^\top \mathbf{B}_d^\top + \mathbf{B}_d \mathbf{W} \mathbf{E}_d^\top + \bar{\epsilon} \mathbf{G}_d \mathbf{G}_d^\top \\ \Theta &:= \mathbf{R}^\top \mathbf{A}_a^\top + \mathbf{A}_a \mathbf{R} + \bar{\epsilon} \mathbf{G}_a \mathbf{G}_a^\top \end{aligned}$$

- matrices \mathbf{H}_d^d , \mathbf{H}_a^d , \mathbf{H}_d^a , and \mathbf{H}_a^a bound the functions $\tilde{\mathbf{f}}_d(\cdot)$ and $\tilde{\mathbf{f}}_a(\cdot)$;
- controller gain is given as $\boxed{\mathbf{K}_d := \mathbf{W} \mathbf{X}^{-1}}$.

- \mathbf{P} is a convex semidefinite program (SDP) that can be solved via a variety of convex programming tools;

The extended version of this manuscript [12] presents theoretical motivations to solve \mathbf{P} , the corresponding mathematical proofs, and more details including the non-restrictive assumptions (boundedness of the vector valued nonlinearities). In short, after solving \mathbf{P} for matrix \mathbf{K}_d , the NDAE (13) can be shown to be asymptotically stable. That is, we show that under this control law $\lim_{t \rightarrow \infty} \|\tilde{\mathbf{x}}_d(t)\|_2 = 0$ and $\lim_{t \rightarrow \infty} \|\tilde{\mathbf{x}}_a(t)\|_2 = 0$.

V. NUMERICAL EXPERIMENTS

A. Simulation Parameters & Setup

This section focuses on comparing the aforementioned methods to perform LFC on the modified IEEE 14-bus network. The network is comprised of 14 buses, 5 generators with $\mathcal{G} = \{1, 2, 3, 6, 8\}$, and 11 loads. All numerical simulations are performed using MATLAB R2020b running on a 64-bit Windows 10 with a 3.0GHz AMD Ryzen™ 9 4900HS processor and 16 GB of RAM, whereas all convex SDPs are solved through YALMIP [19] optimization interface along with MOSEK [20] solver. The NDAE model of the power network is simulated using MATLAB's index-one DAEs solver `ode15i`. All electrical loads are assumed to be of constant power type. For renewable power plants—such as wind farms and solar PVs—are simply modeled as loads with *negative* power, thereby injecting active power to the network. The initial conditions as well as steady-state values of the power network before any disturbance is applied are computed from the solutions of power flow equations, which is obtained from MATPOWER [21] function `rmpf`. The power base for this system is 100 MVA. The synchronous generator parameters are obtained from Power System Toolbox (PST) [11]. The regulation and chest time constants are set to be $R_{Di} = 0.02 \text{ Hz/pu}$ and $T_{CHi} = 0.2 \text{ sec}$, respectively [7].

B. Limitations of Linearization-Based Controllers

In the first instances of numerical simulations, we study the performance of LQR, AGC, and \mathcal{H}_∞ controllers to stabilize the system following a step disturbance, which is triggered by a sudden step change in power generation and demand. The AGC is implemented with K_G chosen to be equal to 1000 (see [12, Section IV-B]). The internal filed voltage for each generator when AGC is used is computed with the aid from the LQR control. The LQR cost matrices are set to $\mathbf{Q} = \mathbf{I}$ and $\mathbf{R} = \mathbf{I}$. The controller gain matrix for the robust \mathcal{H}_∞ control is obtained from solving (11) with $Z_x = 10^{-1} \mathbf{I}$ and $Z_u = 10^{-2} \mathbf{1}$.

The numerical simulations are performed by executing the following steps. Initially, the system operates with total load of $P_L^0 = 2.59 \text{ pu}$ and $Q_L^0 = 0.735 \text{ pu}$ and total generated power from renewables of $P_R^0 = -0.6243 \text{ pu}$ (the negative sign indicates that the power is produced instead of consumed) and $Q_R^0 = 0 \text{ pu}$. Immediately after $t > 0$, the loads and renewables are experiencing an abrupt step change in the amount of consumed and produced power, which triggers a sudden shift in the system's equilibrium. The controller then tries to bring the system frequency back to 60 Hz. The new value of complex power for loads and renewables are specified as $(1 + \rho_L)(P_L^0 + jQ_L^0)$ and $(1 - \rho_R)(P_R^0 + jQ_R^0)$ (these translate to

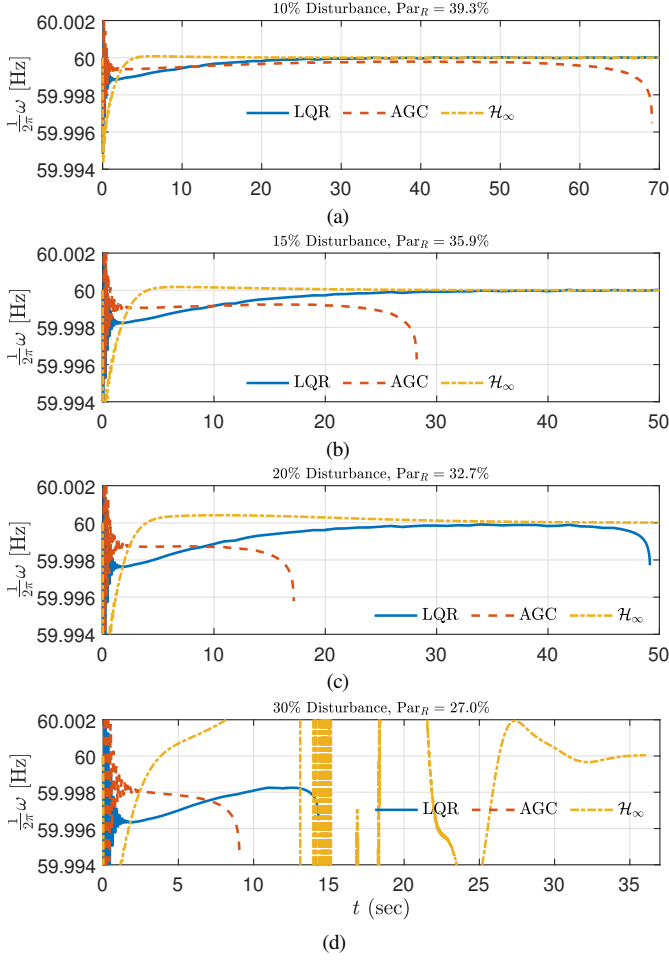


Figure 1. The normalized rotor speed (frequency) of Generator 1 with respect to different levels of disturbance with LQR, AGC, and robust \mathcal{H}_∞ control.

the addition of loads and the reduction of generation from renewables) where $\rho_L, \rho_R \in \mathbb{R}$ determine the quantity of the disturbance. The amount of disturbance acting on the loads and renewables is varied with five different levels ranging from 10% to 30% such that $\rho_L \in \{0.10, 0.15, 0.20, 0.30\}$ and $\rho_R \in \{0.10, 0.15, 0.20, 0.30\}$. Here we define Par_R as the percentage of (average) real power generated by renewables, which gives a numerical figure for the amount of renewables participation and is formulated as

$$\text{Par}_R = \text{average} \left(\frac{\sum_{i \in \mathcal{R}} P_{\text{R}i}(t)}{\sum_{i \in \mathcal{G}} P_{\text{G}i}(t) + \sum_{i \in \mathcal{R}} P_{\text{R}i}(t)} \right) \times 100\%,$$

where $P_{\text{G}i}$ for all $i \in \mathcal{G}$ is computed from the solution of (12) using the proposed linearization-free controller—see Section V-C. At steady state (before the disturbance is applied), $\text{Par}_R = 46.9\%$. Five buses are connected to renewables such that $\mathcal{R} = \{2, 3, 4, 9, 14\}$. It is assumed that the power generated by the renewables contains random Gaussian noise with zero mean and variance of $0.01(P_{\text{R}i}^0 + jQ_{\text{R}i}^0)$ for each $i \in \mathcal{R}$ such that

$$P_{\text{R}i}^e + jQ_{\text{R}i}^e := (1 + \rho_R)(P_{\text{R}i}^0 + jQ_{\text{R}i}^0) + (1 + j)v_i(t), \forall i \in \mathcal{R},$$

where $v_i(t)$ represents the noise associated with $i \in \mathcal{R}$.

The simulation results are given in Fig. 1, where it is shown the resulting frequency of Generator 1 (in Hz). It appears that these controllers fail to stabilize the frequency when the disturbance is large. In particular, the AGC, LQR, and \mathcal{H}_∞ control fail when the

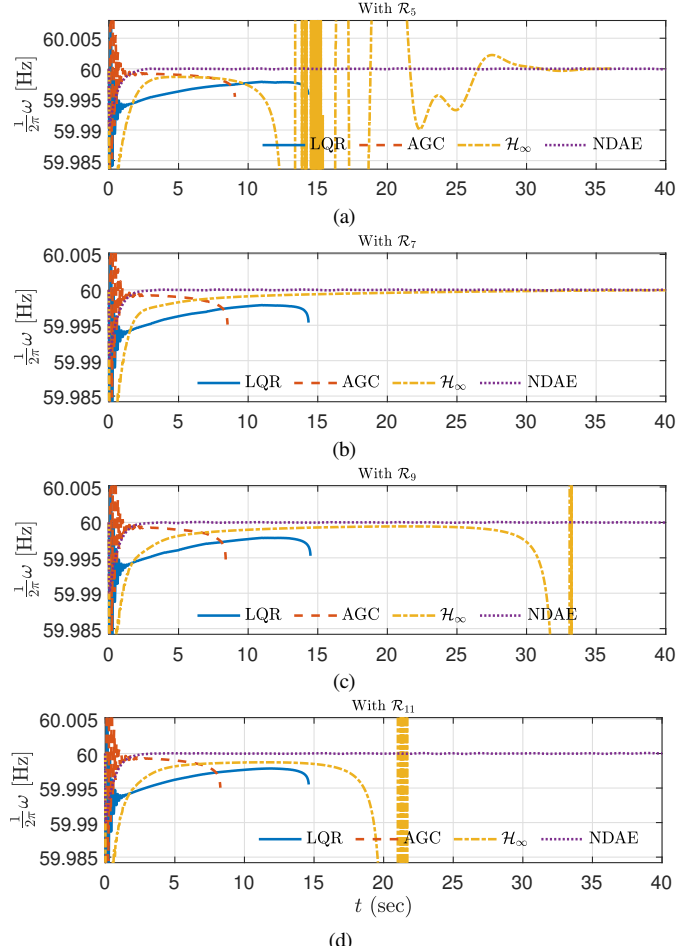


Figure 2. The normalized rotor speed (frequency) of Generator 3 with 30% disturbance and different configurations of renewables.

disturbance is larger than 10%, 20%, and 30%, respectively. This indicates that the AGC performs worst among the three controllers since it cannot handle 10% of disturbance level while, in contrast, the \mathcal{H}_∞ control performs the best due to its ability in preserving frequency stability against 20% disturbance.

C. Linearization-Free vs Linearization-Based Controllers

Herein we showcase the proposed linearization-free controller developed using the NDAE representation of power networks—referred to as the NDAE control from now on—in maintaining the frequency despite the variety of disturbances. The controller gain for the NDAE control is obtained from solving problem \mathbf{P} with $\kappa = 10^{-3}$. The bounding matrices for $\mathbf{f}_d(\cdot)$ and $\mathbf{f}_a(\cdot)$ are chosen to be

$$(\mathbf{H}_d^d)^2 = \mathbf{I}, (\mathbf{H}_a^d)^2 = \mathbf{I}, (\mathbf{H}_d^a)^2 = \mathbf{I}, (\mathbf{H}_a^a)^2 = \mathbf{I}.$$

In this simulation, we consider a high disturbance level such that $\rho_L \in \{0.30\}$ and $\rho_R \in \{0.30\}$. In addition to this, we also consider four distinct locations with different number of renewables that are exist in the network specified as $\mathcal{R}_5 = \{2, 3, 4, 9, 14\}$, $\mathcal{R}_7 = \mathcal{R}_5 \cup \{6, 13\}$, $\mathcal{R}_9 = \mathcal{R}_7 \cup \{5, 10\}$, $\mathcal{R}_{11} = \mathcal{R}_7 \cup \{11, 12\}$ (notice that the subscript index i indicates the number of renewables for any given \mathcal{R}_i).

Fig. 2 shows the rotor speed trajectory of Generator 3 with different penetration levels of renewables and 30% disturbance

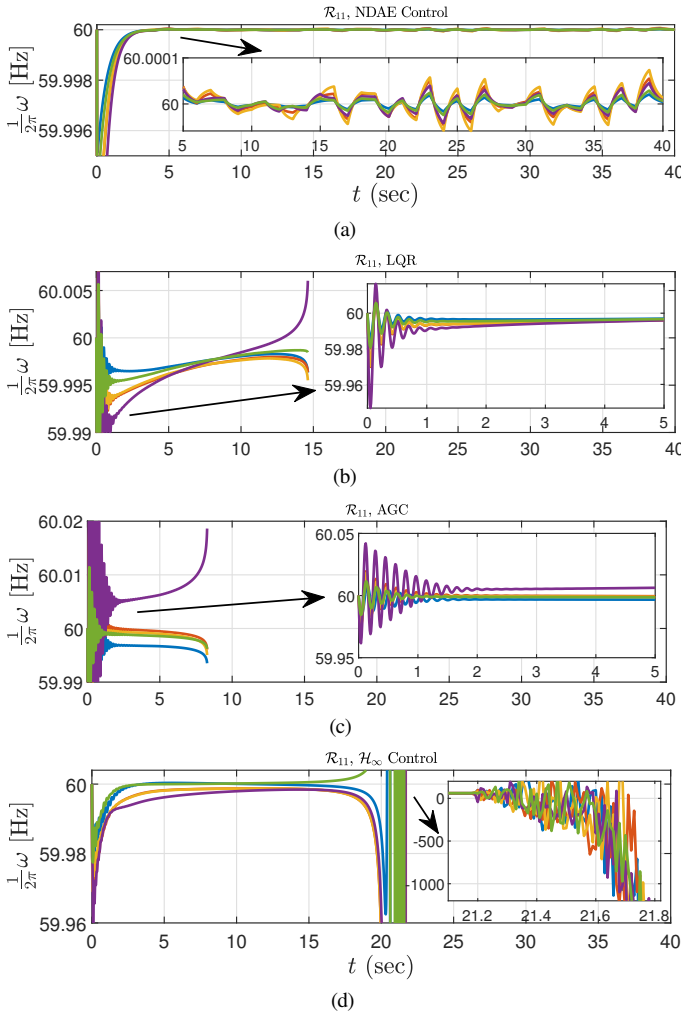


Figure 3. All generators' rotor speed with 11 renewables connected to the grid (\mathcal{R}_{11}) and 30% disturbance level.

level. Notice that neither AGC nor LQR is able to stabilize the network—likewise the robust \mathcal{H}_∞ control, although it is able to do so only when the renewables are configured with \mathcal{R}_7 . However, the proposed controller is able to control the frequencies for all cases. The trajectories of all generators' rotor speed with \mathcal{R}_{11} are depicted in Fig. 3. Notice that only the proposed NDAE controller is able to maintain system-wide stability—this is indicated by the converging generators' rotor speed to the nominal value. The oscillations of generators' rotor speed shown in Fig. (3a) are caused by the noise. More results are included in [12].

VI. PAPER SUMMARY, LIMITATIONS, AND FUTURE WORK

The paper offers an educational summary of multi-machine power network models and the most commonly used linear system theory control algorithms for LFC and frequency regulation. We showcase how and when such algorithms fail in stabilizing power network models and offer simple solution based on nonlinear DAE system theory and convex programming. We demonstrate that the proposed solution outperforms the vintage control theoretic methods, enabling a more robust notion of grid stability amidst significant uncertainty from loads and renewables.

We notice in the simulations that the proposed control law of NDAEs is in fact sparse: the controller gain only requires local measurements from each measurements. We also point out here that a more robust version of the proposed LFC has the potential to perform better. Future work will focus on these investigations and incorporating dynamic models of renewables.

REFERENCES

- [1] Xiaofeng Yu and K. Tomovic, "Application of linear matrix inequalities for load frequency control with communication delays," *IEEE Transactions on Power Systems*, vol. 19, no. 3, pp. 1508–1515, 2004.
- [2] L. D. Marinovici, J. Lian, K. Kalsi, P. Du, and M. Elizondo, "Distributed hierarchical control architecture for transient dynamics improvement in power systems," *IEEE Transactions on Power Systems*, vol. 28, no. 3, pp. 3065–3074, 2013.
- [3] C. E. Fosha and O. I. Elgerd, "The megawatt-frequency control problem: A new approach via optimal control theory," *IEEE Transactions on Power Apparatus and Systems*, vol. PAS-89, no. 4, pp. 563–577, 1970.
- [4] E. Tacker, C. Lee, T. Reddoch, T. Tan, and P. Julich, "Optimal control of interconnected, electric energy systems—a new formulation," *Proceedings of the IEEE*, vol. 60, no. 10, pp. 1239–1241, 1972.
- [5] M. Bazrafshan, N. Gatsis, A. F. Taha, and J. A. Taylor, "Coupling load-following control with opf," *IEEE Transactions on Smart Grid*, vol. 10, no. 3, pp. 2495–2506, 2019.
- [6] N. Chuang, "Robust H_∞ load frequency control in interconnected power systems," in *2013 Australasian Universities Power Engineering Conference (AUPEC)*, 2013, pp. 1–6.
- [7] A. F. Taha, M. Bazrafshan, S. A. Nugroho, N. Gatsis, and J. Qi, "Robust control for renewable-integrated power networks considering input bound constraints and worst case uncertainty measure," *IEEE Transactions on Control of Network Systems*, vol. 6, no. 3, pp. 1210–1222, 2019.
- [8] T. Sadamoto, A. Chakrabortty, T. Ishizaki, and J. Imura, "Dynamic modeling, stability, and control of power systems with distributed energy resources: Handling faults using two control methods in tandem," *IEEE Control Systems Magazine*, vol. 39, no. 2, pp. 34–65, 2019.
- [9] Z. Wang, F. Liu, J. Z. F. Pang, S. H. Low, and S. Mei, "Distributed optimal frequency control considering a nonlinear network-preserving model," *IEEE Transactions on Power Systems*, vol. 34, no. 1, pp. 76–86, 2019.
- [10] D. D. Siljak, D. M. Stipanovic, and A. I. Zecevic, "Robust decentralized turbine/governor control using linear matrix inequalities," *IEEE Transactions on Power Systems*, vol. 17, no. 3, pp. 715–722, 2002.
- [11] P. Sauer, M. Pai, and J. Chow, *Power System Dynamics and Stability: With Synchrophasor Measurement and Power System Toolbox*, ser. Wiley - IEEE. Wiley, 2017.
- [12] S. A. Nugroho and A. F. Taha. (2021) Load and renewable-following control of linearization-free differential algebraic equation power system models. [Online]. Available: <https://arxiv.org/abs/2104.05957>
- [13] E. Mallada and A. Tang, "Dynamics-aware optimal power flow," in *52nd IEEE Conference on Decision and Control*, 2013, pp. 1646–1652.
- [14] B.-M. Hodge, A. Florita, K. Orwig, D. Lew, and M. Milligan, "Comparison of wind power and load forecasting error distributions," National Renewable Energy Lab.(NREL), Golden, CO (United States), Tech. Rep., 2012.
- [15] T. Faulwasser, A. Engelmann, T. Mühlpfordt, and V. Hagenmeyer, "Optimal power flow: an introduction to predictive, distributed and stochastic control challenges," *at - Automatisierungstechnik*, vol. 66, no. 7, pp. 573–589, 2018.
- [16] B. D. Anderson and J. B. Moore, *Optimal control: linear quadratic methods*. Courier Corporation, 2007.
- [17] J. Doyle, A. Packard, and K. Zhou, "Review of lfts, lmis, and mu," in *[1991] Proceedings of the 30th IEEE Conference on Decision and Control*, 1991, pp. 1227–1232 vol.2.
- [18] S. Boyd, L. El Ghaoui, E. Feron, and V. Balakrishnan, *Linear matrix inequalities in system and control theory*. SIAM, 1994.
- [19] J. Löfberg, "Yalmip : A toolbox for modeling and optimization in matlab," in *In Proceedings of the CACSD Conference*, Taipei, Taiwan, 2004.
- [20] E. D. Andersen and K. D. Andersen, *The Mosek Interior Point Optimizer for Linear Programming: An Implementation of the Homogeneous Algorithm*. Boston, MA: Springer US, 2000, pp. 197–232.
- [21] R. D. Zimmerman, C. E. Murillo-Sánchez, and R. J. Thomas, "Matpower: Steady-state operations, planning, and analysis tools for power systems research and education," *IEEE Transactions on Power Systems*, vol. 26, no. 1, pp. 12–19, 2011.